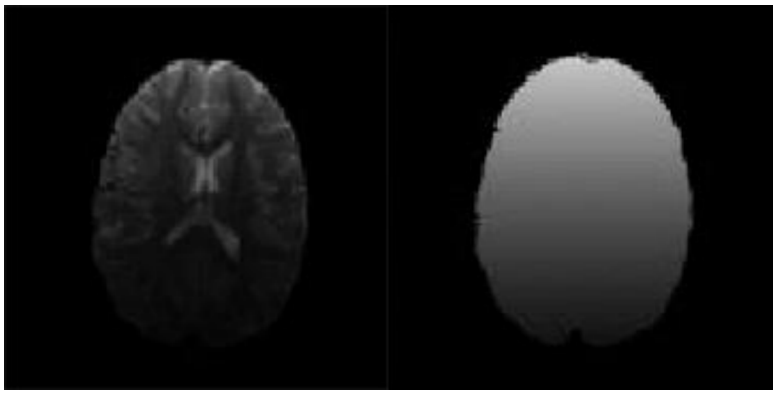

Figure 1. Intensity inhomogeneities in brain MR imaging.

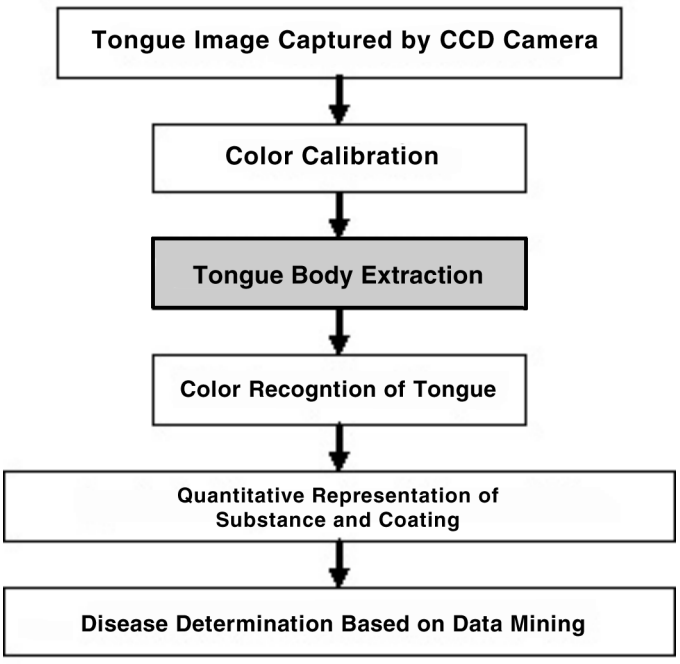

Figure 2. Flowchart of a typical automatic tongue diagnosis system.

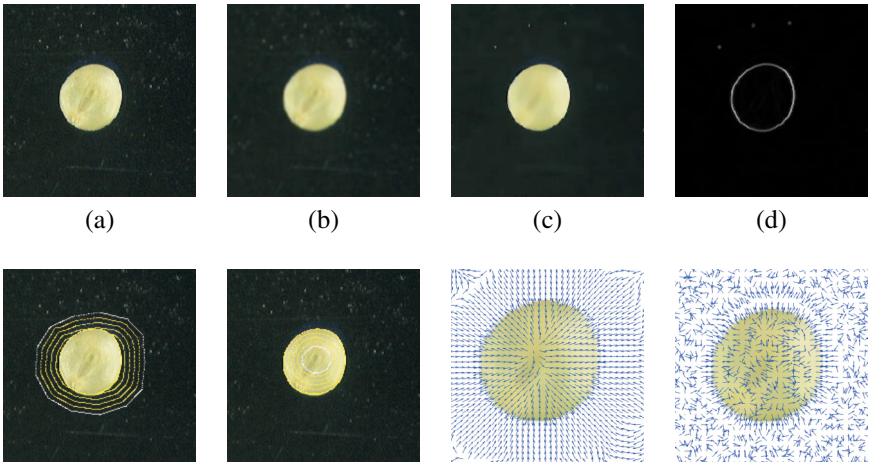

Figure 3. An example of segmenting a seed image using a color GVF snake: (a) original color seed image; (b,c) filtering results from Gaussian kernel and anisotropic diffusion, respectively; (d) edge map using a Di Zenzo color gradient operator; (e,f) convergence of two color GVF snakes with different initial curves; (g,h) closeups of external force fields in a color GVF snake and a classical snake, respectively.

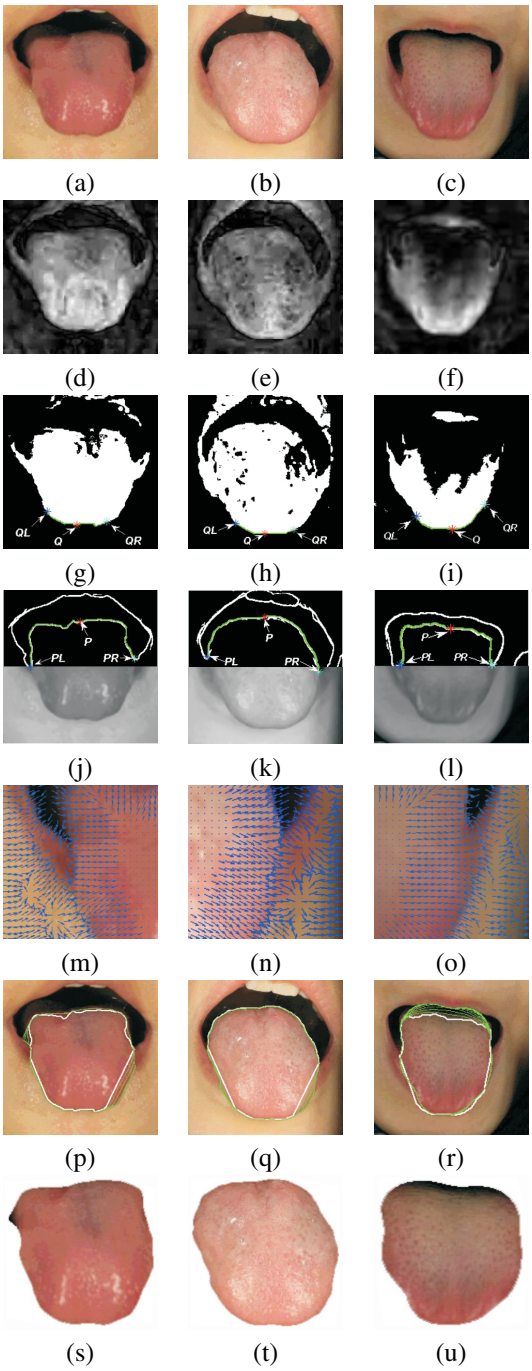

Figure 4. Extraction of tongue bodies using the color GVF Snake on three tongue images. Each column shows an example of tongue segmentation.

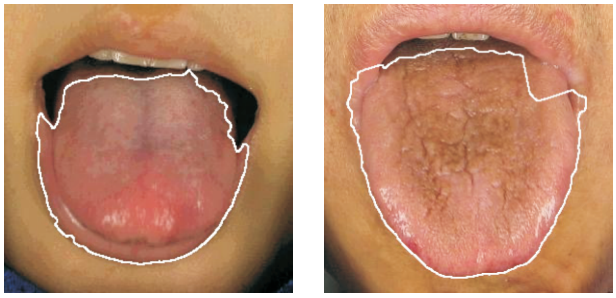

(a) (b)

Figure 5. Two failure examples of tongue image segmentation by snakes. Notice the white curves are the boundary-finding results.

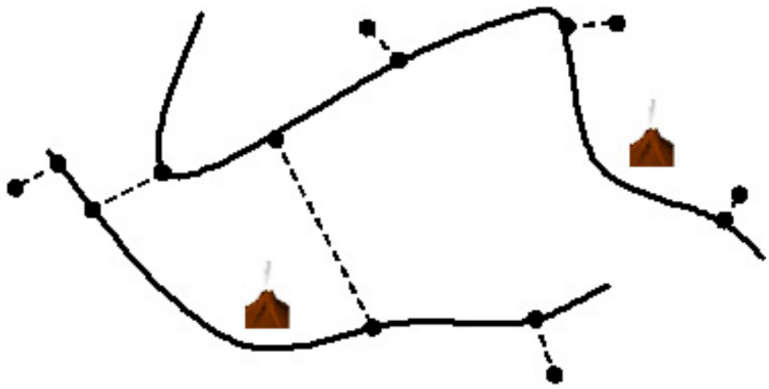

Figure 6. Geometric interpretation of Snake Pit. The two dark curves are different snakes, and the tow springs (dashed line) are connected between them to create a coupling effect. The other springs attach points on the snakes to fixed positions in the image. In addition, two volcanos are set to bend a nearby snake.

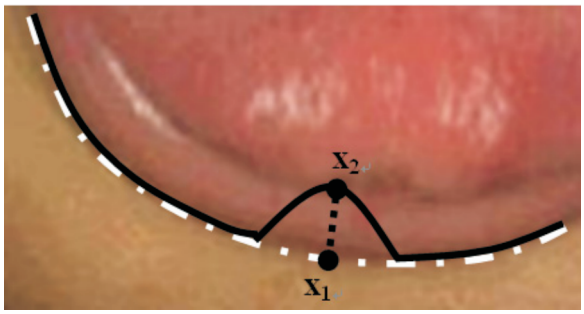

Figure 7. A pair of points for the snake pit.

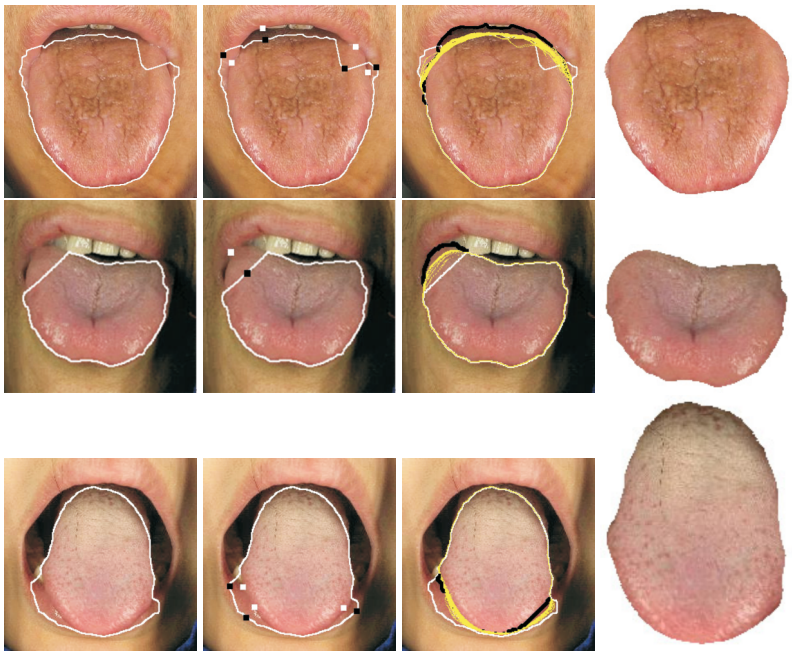

Figure 8. Examples of interactive segmentation on three tongue images. The four columns from left to right are: original segmentation results from the color GVF snakes, point pairs chosen for the snake pit, convergence of the snakes, and final extracted tongue bodies.

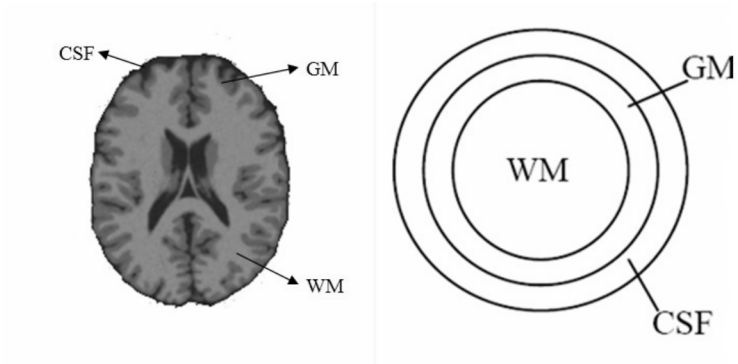

Figure 9. Left: transversal slice of MR brain volume constituting WM, GM, and CSF, as labeled. Right: simplified model with ribbon-like structure. While real cerebral cortex has varying thickness, it is approximated with constant thickness in the simplified model. The motivation for this simplification will be discussed in more depth below.

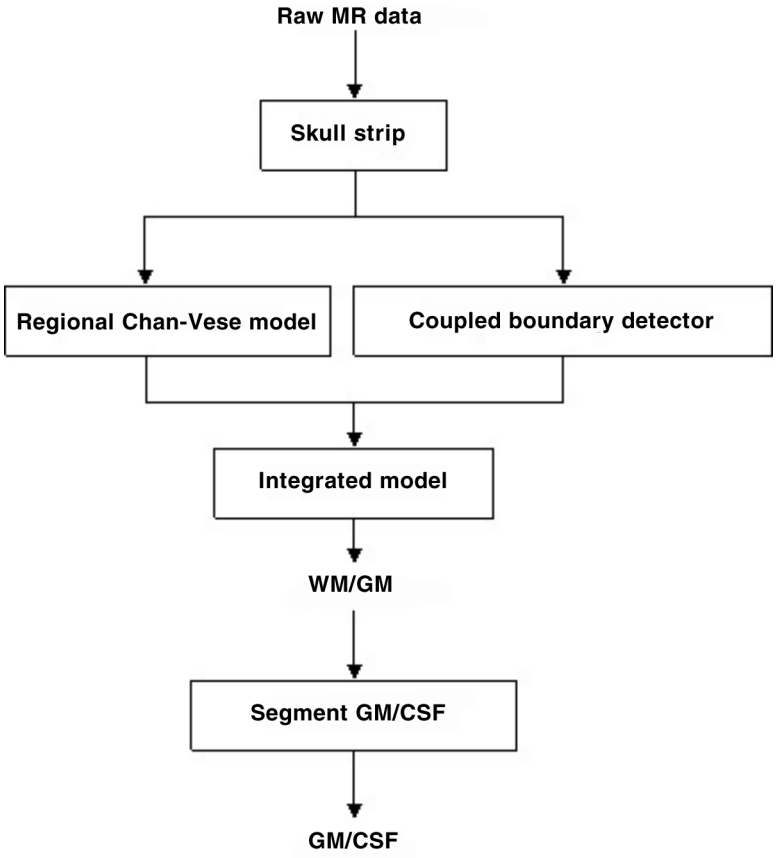

Figure 10. Block diagram of the entire system.

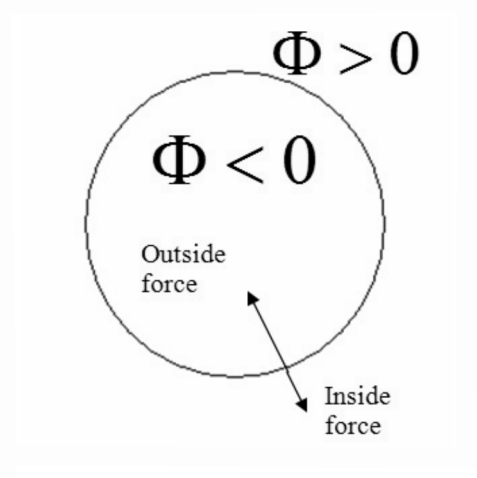

Figure 11. The entire plane is decomposed by the evolving curve into two regions, with $\Phi > 0$ for the outer and $\Phi < 0$ for the inner region. The evolving curve is characterized by $\Phi = 0$. During evolution of the curve, the inside and outside forces compete to determine the speed and direction of curve propagation until a balance between these two forces is established.

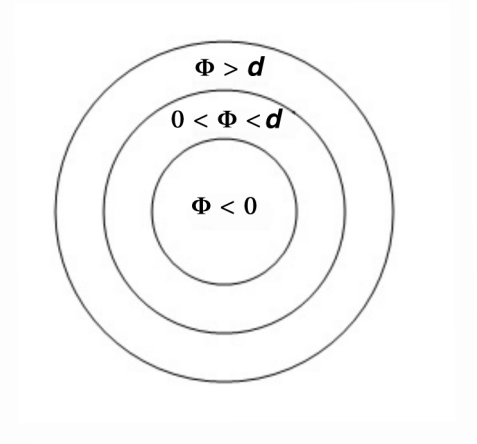

Figure 12. The brain can be simplified and modeled as three concentric spheres (or circles in 2D). The areas of $\Phi < 0$, $0 < \Phi < d$, and $\Phi > d$ represent the WM, GM, and CSF respectively.

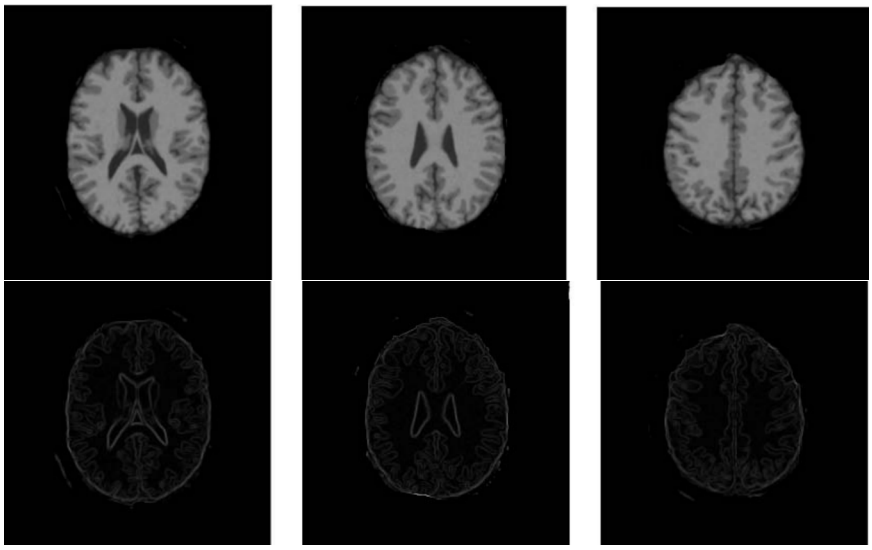

Figure 13. Results from image gradient operators. Top: slices from the original MR data. Bottom: results from a gradient operator.

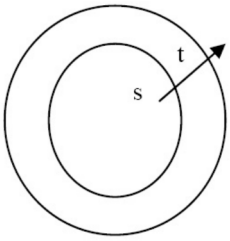

Figure 14. The coupled boundary is defined by a set of coupled points s and t.

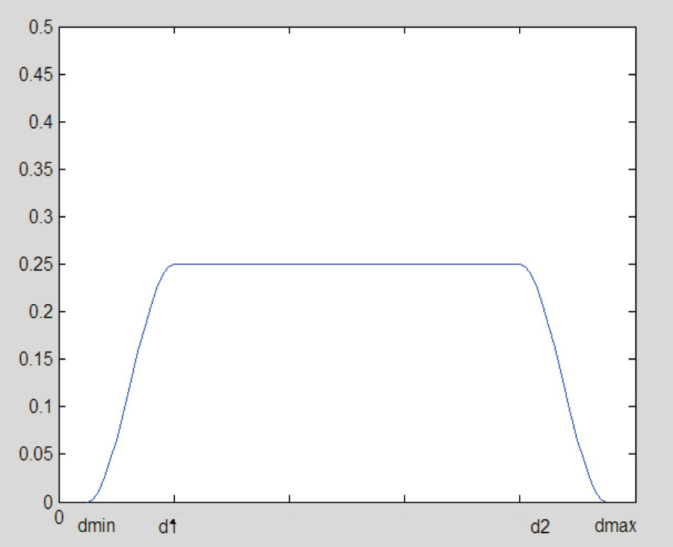

Figure 15. Function h used as a prior constraint: $d_{\min}$ = minimum distance allowed; $d_{\max}$ = maximum distance allowed.

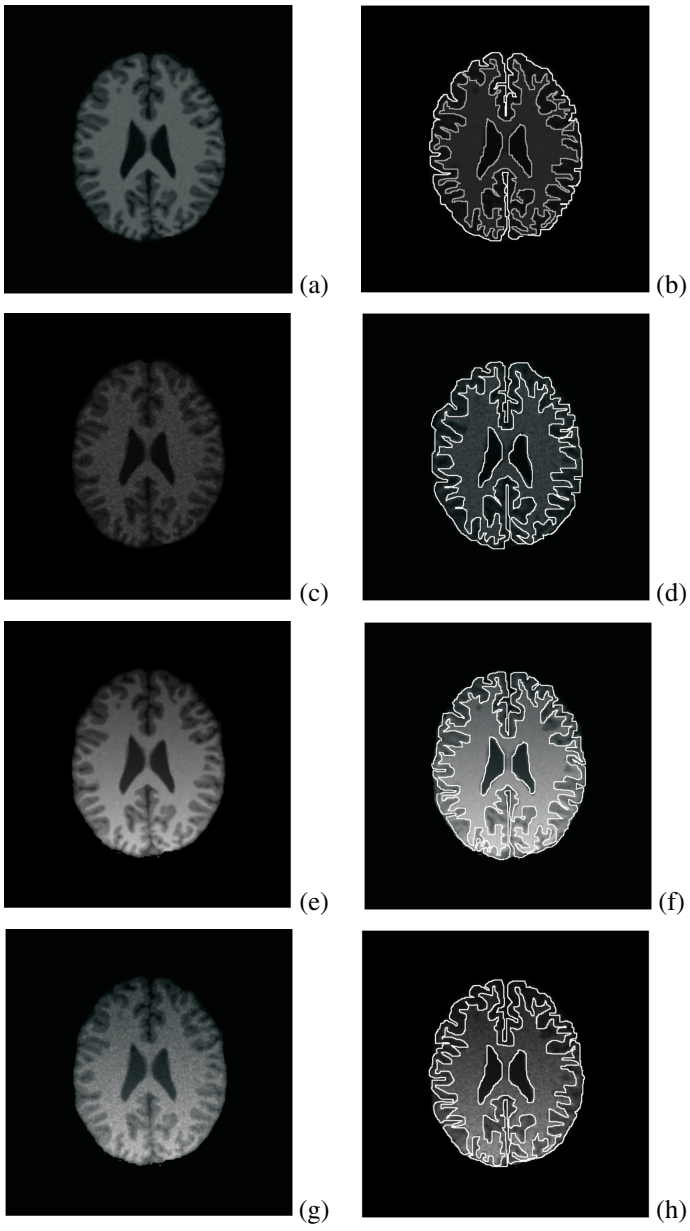

Figure 16. Results on simulated data with our method for four cases. Left: axial slices of original data. Right: automatically detected contours on axial slices. (a,b) noise = 3%, intensity inhomogeities = 0%; (c,d) noise = 9%, intensity inhomogeities = 0%; (e,f) noise = 3%, intensity inhomogeities = 40%; (g,h) noise = 9%, intensity inhomogeities = 40%.

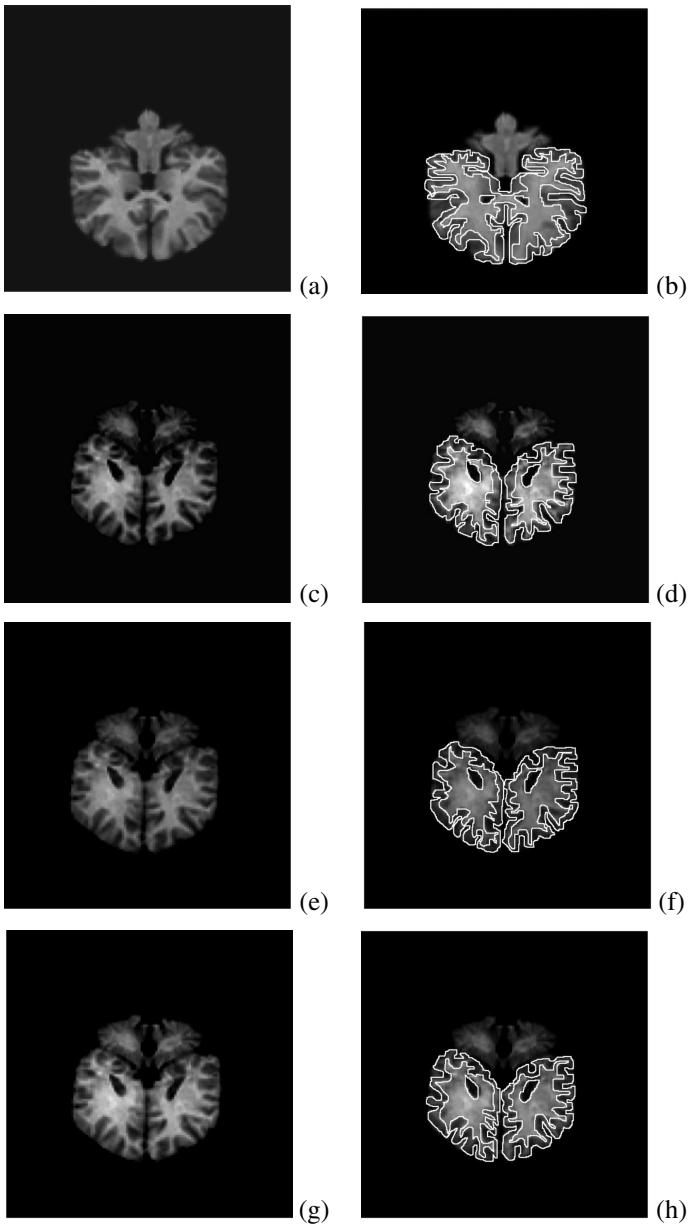

Figure 17. Result on 20 normal T1-weighted brains using our method. Left: coronal slices from original data. Right: automatically detected contours on coronal slices. (a,b) 100_23; (c,d) 111_2; (e,f) 13_3; (g,h) 7_8.

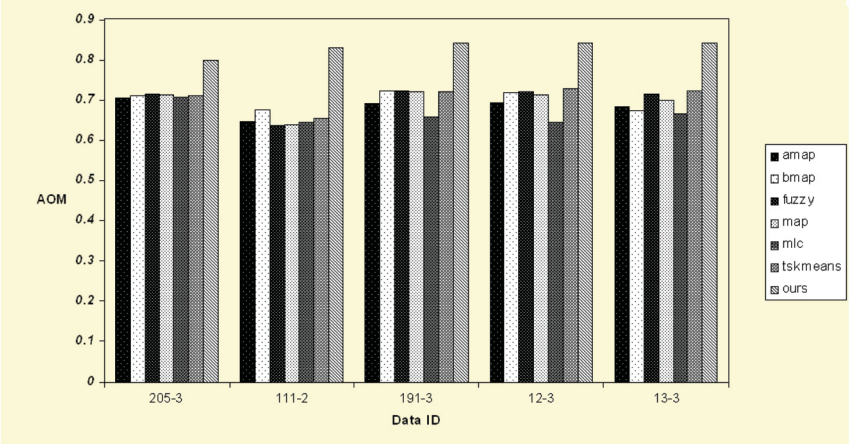

Figure 18. AOM on 20 normal T1-weighted brains for WM segmentation using various methods.

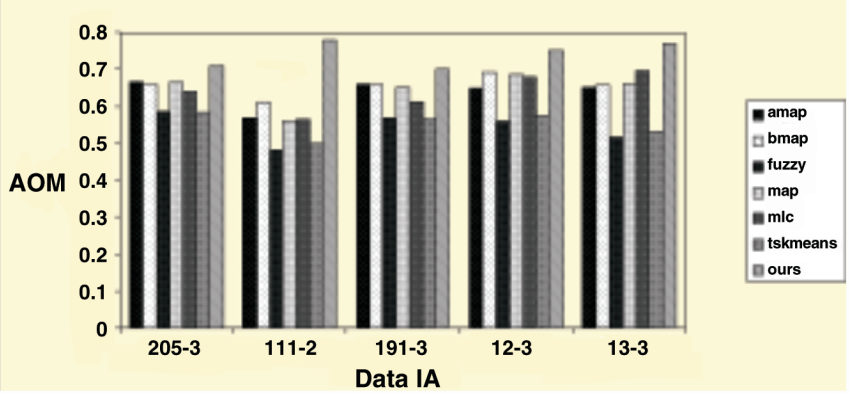

Figure 19. AOM on 20 normal T1-weighted brains for GM segmentation from various methods.

(a) (b) (c)

Figure 20. Cardiac valve segmented by region prior-based geodesic snake: (a) image from an echocardiographic sequence and the prior valve region; (b) result of preprocessing; (c) final segmenting result with region prior-based geodesic snake.

(a) (b) (c) (d)

Figure 21. Circle segmented by the shape prior-based geodesic snake: (a) circle stained by a bar and salt-and-pepper noise; (b) circle segmented by the geodesic snake; (c) prior circle shape; (d) circle segmented by shape prior-based geodesic snake.

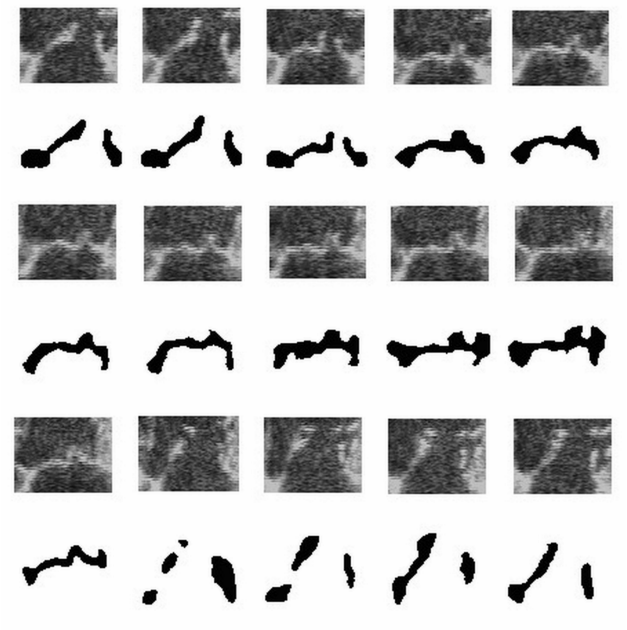

Figure 22. Valves segmented using the region prior-based geodesic snake.

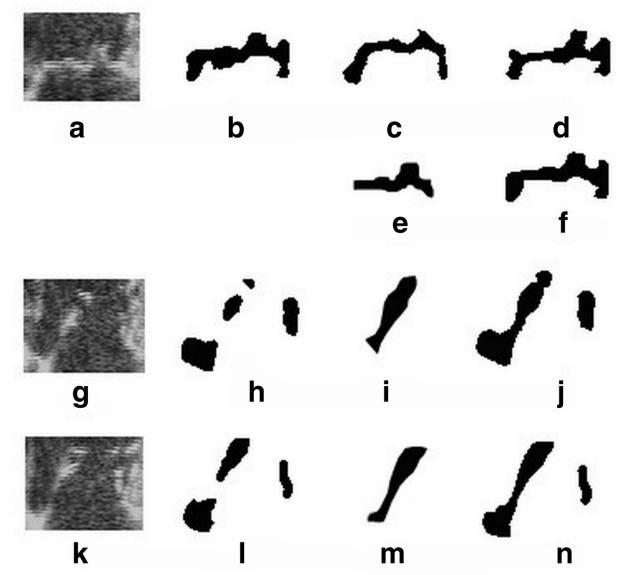

Figure 23. Cardiac valve segmented by the shape prior-based geodesic snake: (a,g,k) initial echocardiographic image; (b,h,l) result guided by region prior; (c) segmentation result of neighbor slice; (d) result guided by shape prior of (c); (e,i,m) manual outline; (f,j,n) result guided by shape prior.